nature communications

Article

https://doi.org/10.1038/s41467-024-53922-x

The massed-spaced learning effect in non-neural human cells

Received: 21 February 2024

Accepted: 28 October 2024

Published online: 07 November 2024

Check for updates

N. V. Kukushkin[1,2,3] ✉, R. E. Carney[2], T. Tabassum[2] & T. J. Carew[2,3] ✉

The massed-spaced effect is a hallmark feature of memory formation. We now demonstrate this effect in two separate non-neural, immortalized cell lines stably expressing a short-lived luciferase reporter controlled by a CREB-dependent promoter. We emulate training using repeated pulses of forskolin and/or phorbol ester, and, as a proxy for memory, measure luciferase expression at various points after training. Four spaced pulses of either agonist elicit stronger and more sustained luciferase expression than a single "massed" pulse. Spaced pulses also result in stronger and more sustained activation of molecular factors critical for memory formation, ERK and CREB, and inhibition of ERK or CREB blocks the massed-spaced effect. Our findings show that canonical features of memory do not necessarily depend on neural circuitry, but can be embedded in the dynamics of signaling cascades conserved across different cell types.

Learning and memory in animals exhibit a peculiar feature known as the massed-spaced effect: training distributed across multiple sessions (spaced training) produces stronger memory than the same amount of training applied in a single episode (massed training). This effect is highly conserved across the animal kingdom and is observed at both behavioral and synaptic levels[1–10].

The massed-spaced effect, also known as the spacing effect and first documented by Hermann Ebbinghaus[11], is characterized by the existence of an optimal intertrial interval (ITI) between training sessions. Previous research has identified some molecular and cellular components that determine this optimal spacing[12]. For instance, studies in *Drosophila* have shown that manipulating SHP2 expression in mushroom body neurons alters the optimal ITI for long-term memory (LTM) induction, correlating with changes in the activation of extracellularly regulated kinase (ERK)[13]. Similarly, our research in *Aplysia* has demonstrated a correlation between ERK phosphorylation timing and optimal spacing of training patterns[14–16].

While the spacing effect is typically associated with neural systems, we hypothesized that it might also be observable in non-neural cells, given that much of the molecular toolkit for memory formation is conserved across cell types (Fig. 1). To test this hypothesis, we developed a non-neural reporter cell line to study the spacing effect. On the one hand, it provides exponentially greater experimental throughput than neural systems, accelerating the development of formal, predictive models of memory formation, and in the future, potentially creating new avenues for cognitive enhancement and treatment of cognitive disabilities. On the other hand, it enables the exploration of "cellular cognition" beyond neural systems.

Our study builds upon previous work on temporal pattern detection by individual neurons[5,16,17], including those expressing CRE reporters[18], the emergent properties of biological cascades in non-neuronal cells[19], including research on bistable switch-like behaviors in ERK signaling[20–24], and models of how different effects of massed vs. spaced stimulation could lead to different learning outcomes[25]. What is distinct in our approach is the exposure of generic, non-neural cell cultures to fast, minute-scale temporal patterns generally believed to be the province of neurons.

Results

Design and calibration of a reporter cell line

We developed our reporter system from the human neuroblastoma cell line, SH-SY5Y. Our choice of input stimuli was motivated by our previous studies of spaced training in *Aplysia* neurons, which employed serotonin (5HT) as the memory-inducing stimulus. 5HT engages multiple conserved signaling cascades, and its effect on memory is known to rely on protein kinases A and C (PKA and

[1]Liberal Studies, New York University, New York, NY 10003, USA. [2]Center for Neural Science, New York University, New York, NY 10003, USA. [3]These authors jointly supervised this work: N. V. Kukushkin, T. J. Carew. ✉e-mail: nk59@nyu.edu; tc71@nyu.edu

https://doi.org/10.1038/s41467-024-53922-x

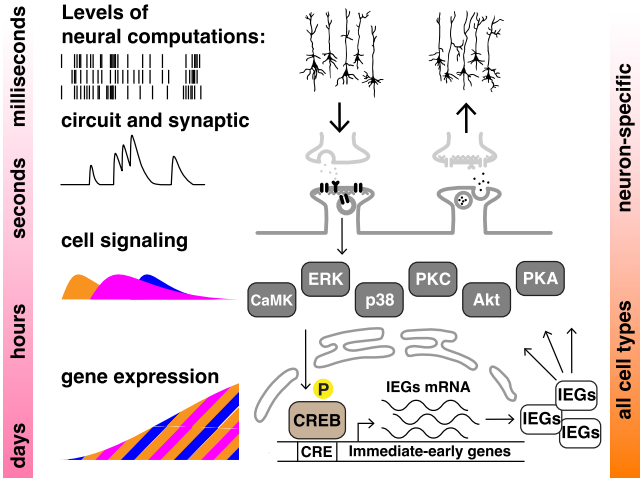

Fig. 1 | Levels of neural computation. Computations are generally taken to occur at the circuit and synaptic levels of neuronal function on the timescales of milliseconds to seconds. These, however, are nested within slower, cellular computations that occur on the levels of cell signaling (seconds to hours) and gene transcription (hours to days and beyond)—*left column*. During long-term memory formation, the transcription factor CREB integrates transient experiential information from various signaling kinases, and modulates the more sustained transcription of cAMP response element (CRE)-dependent immediate-early genes, which modify the function of the neuron for an extended period of time. Although both the inputs and outputs of this system are neuron-specific, the conversion of transient signals into more sustained CRE-dependent transcription can be studied in non-neuronal cells—*right column*.

PKC)[26–29], which, in contrast to 5HT receptors, are common to all eukaryotic cells. We therefore applied activators of PKA and PKC to SH-SY5Y cells in place of 5HT. Forskolin, the activator of adenylate cyclase, was used to raise cellular levels of cyclic adenosine monophosphate (cAMP) and thus activate PKA (Fig. S1). Tetradecanoyl phorbol acetate (TPA) was used as a direct activator of PKC, substituting for its endogenous second messenger diacylglycerol. Phorbol esters and cAMP have indeed been shown to substitute for 5HT in at least some forms of synaptic facilitation in *Aplysia*[16,30].

Our choice of experimental output was also based on the existing understanding of cell signaling in the service of memory formation. It is well known that memory induction in neurons is associated with the transcription of immediate-early genes (IEGs), a large network of early-response genes under the control of a cAMP response element (CRE) and the corresponding transcription factor, cAMP response element-binding protein 1 (CREB1)[31–35]. When CREB1 is phosphorylated by upstream signaling kinases, it drives expression of IEGs, which go on to modify the function of the neuron (Fig. 1 and Fig. S1). Although many IEGs are relatively or completely specific to neurons (e.g. neurotransmitter-producing enzymes and synaptic vesicle proteins), CRE and CREB are conserved across cell types and regulate a diverse range of cellular responses to environmental stimuli. CREB1 is phosphorylated, directly and indirectly, by many key signaling enzymes including PKA, PKC, ERK, p38, Akt, CaMKII and CaMKIV, which in turn receive their inputs from a variety of receptors and second messengers, and in doing so, encode real-time cellular experience. CREB serves as an integrator of this experiential information that converts transient patterns of cell signaling into sustained cellular changes[36,37]. We therefore chose the expression of luciferase placed under the control of CRE as our proxy for cellular memory. To ensure that the readout represents immediate transcriptional activity rather than the accumulation of the protein product, we employed a short-lived variant of luciferase modified with a destabilizing PEST sequence[38] (Fig. 2A). A monoclonal cell line was derived from SH-SY5Y cells stably transfected with a CRE-dependent, PEST-modified luciferase, and termed CRE-luc.

To calibrate our system, we first measured the response of CRE-luc to forskolin and TPA (Fig. 2B, C). Cells were kept in serum-free media for 24 h prior to the start of the experiment. At t = 0, cells were perfused with media containing either of the two agonists in various concentrations, and responses were measured 4 h after the onset of the treatment. Drugs were applied either in a single 3-minute pulse followed by media washout, or continuously throughout the 4 h incubation. Both compounds elicited robust expression of luciferase at t = 4 h. Interestingly, the responses to TPA (Fig. 2C) were roughly similar regardless of the length of treatment, whereas responses to forskolin (Fig. 2B) differed more strongly between the single 3 min pulse and the continuous 4 h incubation, demonstrating higher sensitivity to the treatment duration.

For subsequent experiments, we selected concentrations of both forskolin and TPA that elicited minimal effect after a single pulse of each: forskolin was used at a concentration of 2 μM, and TPA 2 nM. This allowed for a greater dynamic ratio of luciferase induction in response to different *numbers* of pulses.

Repetition boosts CRE-dependent transcription and slows its decay

To mimic our past studies, which employed 5HT acting through both the PKA and PKC signaling cascades[26–29], as closely as possible, we employed a combination of forskolin and TPA delivered simultaneously (Fig. 2E). A single 3-min pulse of this drug combination produced robust luciferase expression 4 h after training. Four pulses of the same (ITI = 10 min) also induced luciferase expression, which was ~1.4-fold higher ($n = 3$). By 24 h, however, luciferase expression induced by a single pulse was reduced, but remained relatively stable in cells that had received four pulses, eventually leading to a 2.8-fold difference between conditions (n = 14). Similar effects were observed for both TPA (Fig. 2F) and forskolin (Fig. 2G) alone. The largest differences between the effects of a single pulse and repeated pulses (29% vs 391% increase compared to untreated controls after 24 h, respectively) were observed for TPA. Notably, the length of TPA treatment had hardly any effect of luciferase expression (Fig. 2C). It appears that while PKA is more sensitive to the duration of stimulation, PKC is more sensitive to the number of events.

It is especially notable that the difference in the induction of luciferase by 1 versus 4 pulses of TPA or TPA+forskolin becomes greatly accentuated at 24 h, even though (i) stimulation in all cases ceases less than 1 h after the onset of the protocol, and (ii) at 4 h, the induction of luciferase is comparable. This result aligns well with the established dynamics of memory formation: repetition influences not only the immediate strength of memory, but the rate of forgetting, and so long-term memory differences between training protocols emerge over time. This phenomenon is most famously expressed in Ebbinghaus's forgetting curves, whose slopes change with every subsequent repetition of training[11]. Our result also demonstrates the utility of the short-lived, PEST-tagged reporter construct, since without a destabilizing sequence it may not have been possible to observe cellular forgetting. Since elevated levels of luciferase can be cleared from the cells by 24 h post-training, their lingering expression in cells treated with 4 pulses of TPA reflects not simply the accumulation of the product, but continued activity of the CRE promoter, and thus, ongoing transcription of IEGs. Notably, we observe continued expression of luciferase well past the brief timeline of immediate-early gene expression typically reported in neural systems. Several explanations are possible. Non-neural cells may contain additional mechanisms for sustained transcriptional induction, or neural cells may possess additional mechanisms restricting such sustained transcription; transcription of different genes may be differentially sustained in time, for example via

https://doi.org/10.1038/s41467-024-53922-x

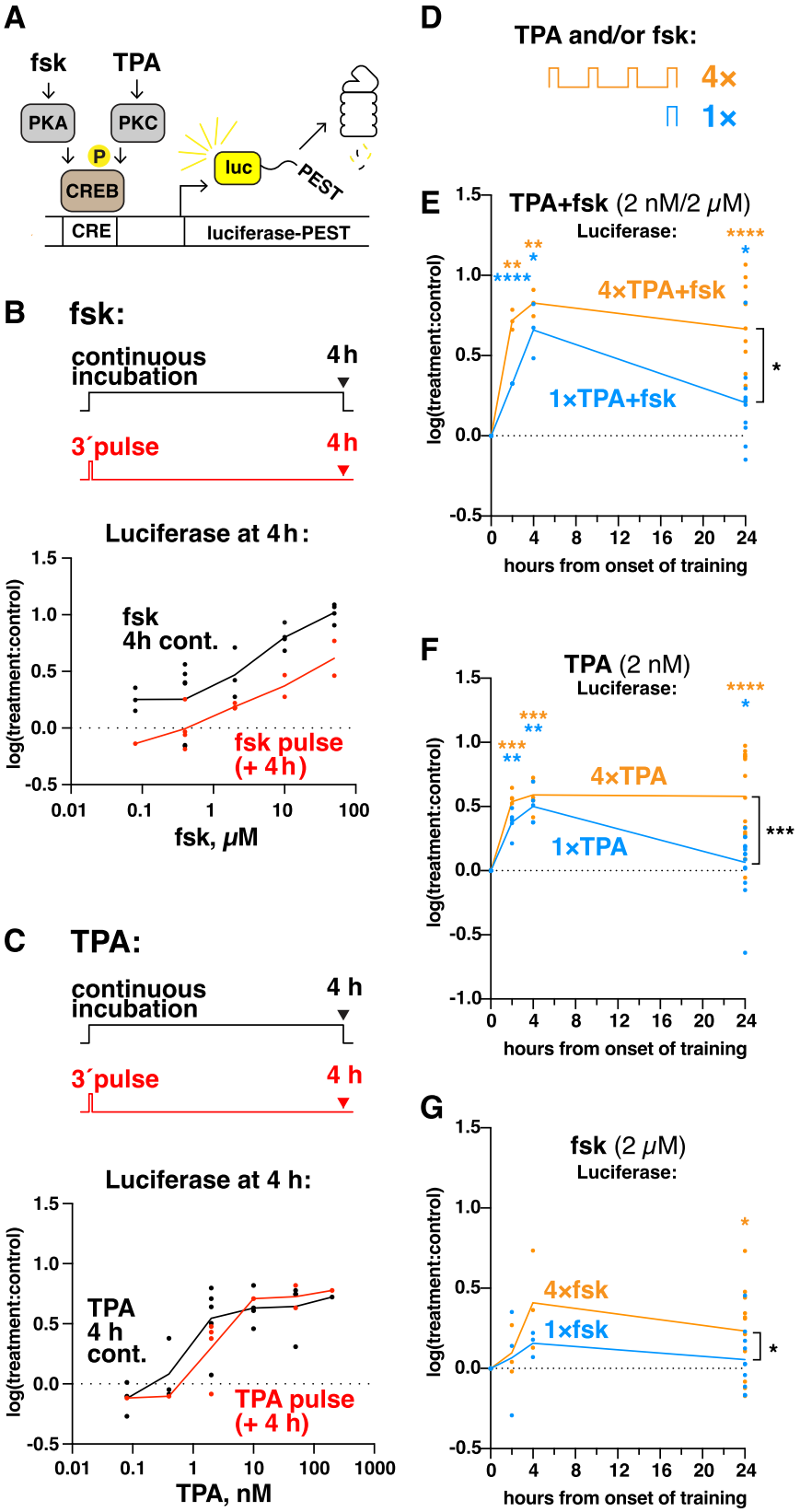

differential transition to transcription independent of CREB phosphorylation[39,40]; stimulation with chemical agonists may elicit much stronger responses than endogenous synaptic stimulation; or, the sensitivity of our system may allow us to observe transcriptional changes more robustly than in neurons. These possibilities warrant further investigation.

CRE-luc cells display the massed-spaced effect

Next, we turned to an examination of the massed-spaced effect. Cells were treated with either a single 3-min pulse of the TPA+forskolin combination, or either drug by itself; four pulses, spaced either 10, 20 or 30 min apart; or a single quadruple 12-min pulse representing the massed condition (Fig. 3A–C). Expression of luciferase was measured 24 h

Fig. 2 | Calibrating the CRE-luc reporter cell line. A Schematic of the reporter. PEST-tagged firefly luciferase is placed under a CRE promoter. Forskolin (fsk) is used to activate PKA, and TPA to activate PKC, leading to increased CRE-luc expression. Levels of luciferase reflect immediate levels of transcriptional induction because the destabilizing PEST sequence leads to rapid proteasomal degradation of luciferase. See also Fig. S1. CRE-luc expression 4 h after the onset treatment with either fsk (**B**) or TPA (**C**) in various concentrations. Treatments were administered either continuously for 4 h (black), or as a single 3-min pulse followed by washout and 4 h recovery (magenta). N represents independent experiments ($N = 1$ for 0.08 μM fsk (3′), 0.08 nM TPA (3′), 0.4 nM TPA (3′), 10 nM TPA (3′), 200 nM TPA (3′), and 200 nM TPA (4 h). $N = 2$ for 10 μM fsk (3′), 50 μM fsk (3′), 50 nM TPA (3′). $N = 3$ for 0.08 μM fsk (4 h), 2 μM fsk (4 h), 0.08 nM TPA (4 h), and 0.4 nM TPA (4 h). $N = 4$ for 0.4 μM fsk (3′), 2 μM fsk (3′), 10 μM fsk (4 h), 50 μM fsk (4 h), 2 nM TPA (3′), 10 nM TPA (4 h), 50 nM TPA (4 h). $N = 5$ for 2 nM TPA (4 h). $N = 6$ for 0.4 μM fsk (4 h)). **D**–**G** fsk and/or TPA were administered either as a single 3 min pulse (blue) or four pulses spaced 10 min (orange), and luciferase expression measured 2, 4 or 24 h from the onset of treatment. **D** Schematic of the treatments; (**E**), combination of TPA and fsk; (**F**), TPA alone; (**G**), fsk alone. Trendlines represent means. N represents independent experiments ($N = 3$ for fsk and TPA+fsk, 2 h and 4 h; $N = 5$ for TPA, 2 h and 4 h; $N = 10$ for 1×fsk, 24 h, $N = 11$ for 4×fsk, 24 h; $N = 14$ for TPA, 24 h. 24 h data points include data from Fig. 3). Asterisks above data points indicate p values in two-tailed single-sample Student's t tests (theoretical mean = 0; 4×fsk 24 h, $p = 0.0199$; 1×TPA 2 h, $p = 0.0011$; 1×TPA 4 h, 0.0011; 4×TPA 2 h, $p = 0.0002$; 4×TPA 4 h, $p = 0.0004$; 4×TPA 24 h, $p < 0.0001$; 1×TPA+fsk 2 h, $p < 0.0001$; 1×TPA +fsk 4 h, $p = 0.0213$; 1×TPA+fsk 24 h, $p = 0.0235$; 4×TPA+fsk 2 h, $p = 0.0024$; 4×TPA +fsk 4 h, $p = 0.032$; 4×TPA+fsk 24 h, $p < 0.0001$). Asterisks between data points indicate p values in two-tailed paired Student's t tests (1×TPA+fsk 24 h vs 4×TPA+fsk 24 h, $p < 0.0001$; 1×TPA 24 h vs 4×TPA 24 h, $p < 0.0001$; 1×fsk 24 h vs 4×fsk 24 h, $p = 0.009$). Summary p values: $^{*}p < 0.05$; $^{**}p < 0.01$; $^{***}p < 0.001$. Source data are provided as a Source Data file.

after treatment. In all cases, expression of luciferase induced by spaced pulses was significantly greater than by the massed treatment. For TPA +forskolin and TPA alone, the optimal ITI was 10 min, and the induction of luciferase diminished with more time between pulses. For forskolin alone, the difference between ITIs was less pronounced, with 20 min being optimal. This suggests that PKA and PKC are "tuned" to distinct ITIs, meaning that responses to neuromodulators such as 5HT may in fact be an interactive summation of these overlapping timelines.

In our previous studies in *Aplysia*, we observed that two events spaced 45 min had the same effect on long-term memory as four events spaced 15 min[14]—in other words, only two events, and their temporal spacing, were critical for the induction of sensitization memory in that system. Although the precise mechanisms for this temporal specificity remain unknown, we tested whether CRE-luc cells also responded to the overall duration of the training protocol, rather than repetition of the training pulses, by including in our experiments two-pulse protocols that matched the timing of the first and last pulse in the four-pulse TPA treatment protocols (Fig. S2). These two-pulse protocols, however, did not induce sustained luciferase expression, indicating that repetition of >2 training pulses is critical for the effect.

To recapitulate, we observed the classic massed-spaced effect and demonstrated the existence of an optimal, non-zero ITI for the induction of maximal memory in CRE-luc cells.

Massed-spaced effect correlates with CREB and ERK activation

To further characterize the massed-spaced effect in CRE-luc cells, we studied the effect of various TPA treatment protocols (1×, 4×, and massed) on the phosphorylation of CREB and ERK, an important node of cellular signaling known to act upstream of CREB and to integrate transient events in the service of long-term memory formation, including signals from PKA and PKC[16,41–44]. Cells were lysed immediately after the end of the training protocol. Western blot showed robust phosphorylation of ERK after all treatments, and CREB after the 4× and massed treatments (Fig. 3D, E). However, both types of phosphorylation were significantly stronger in cells treated with 4 spaced pulses compared to the massed paradigm. We therefore observed the massed-spaced effect at the level of post-translational modifications immediately after the treatment protocol. We conclude that the temporal discrimination between the spaced and massed paradigms occurs at least in part upstream of ERK activation. Notably, when cells were lysed 1, 2, or 4 h after the treatment protocol, the differences in effects between paradigms gradually waned (Fig. S4A), but by 24 h were once again readily apparent (Fig. S4B): although the residual P-ERK elevation was modest (~50% compared to ~600% observed immediately after training), it was only observed in cells that had received the 4×TPA treatment, suggesting that additional mechanisms to differentially sustain ERK phosphorylation may come into play >4 h after training.

At rest, ERK is localized to the cytosol[45]. Upon its phosphorylation, ERK translocates to the nucleus, where it exhibits its principal downstream effects such as the activation of transcription factors including CREB (Fig. S1). To examine whether the spaced and massed paradigms lead to differential translocation of ERK to the nucleus, we studied the localization of total ERK and P-ERK by immunofluorescence immediately after treatment with TPA (Fig. 3F–H and Fig. S5). As expected from our Western blot results, we observed significant induction of ERK phosphorylation by spaced pulses of TPA (Fig. 3F–G). The differences observed between conditions were lower than those seen by Western blot (Fig. 3D–E), but this compression of the effects is explained by significant unspecific binding of the P-ERK antibody. To account for this effect, we employed a 30-min treatment with the ERK phosphorylation inhibitor U0126, which we showed by Western blot to cause an almost complete (~96%) removal of P-ERK (Fig. S5). The density of the P-ERK signal observed by immunofluorescence after an identical U0126 treatment (Fig. 3G) therefore demonstrates the real baseline for ERK-phosphorylation and confirms that immunofluorescence severely underestimates the magnitude of P-ERK changes. Despite this constraint, we did observe a significantly greater nuclear:cytosolic ratio of P-ERK immediately after spaced training compared to massed training (Fig. 3H). The same trend was observed for total ERK (Fig. S7). Overall, both phosphorylation and nuclear translocation of ERK differentially respond to massed and spaced treatments with TPA, indicating that the temporal pattern of stimulation is decoded at least in part either by ERK itself, or upstream of this kinase.

Similarly to the P-ERK/total ERK ratio, the ratio of P-CREB to total CREB 24 h after training was also significantly different between training paradigms and highest in 4×TPA-treated cells (Fig. S4B). The P-CREB/total CREB ratio was only slightly elevated above baseline after the 4×TPA treatment, and instead it was reduced below baseline in cells that had received suboptimal training (1×TPA and massed TPA). At the same time, we observed a modest increase in total CREB protein in 4×TPA-treated cells but not in 1×TPA or massed-treated cells. When the two effects (on P-CREB/total CREB ratio and on total CREB protein) were multiplied (accounting, therefore, for absolute levels of S133 P-CREB 24 h after training), the product, in 4×TPA-treated cells, was robustly above baseline and significantly greater than in other paradigms (Fig. S4B). These results suggest that CREB-dependent transcription is regulated not only via CREB phosphorylation, but also by controlling the levels of total CREB protein, and both effects are preferentially induced by spaced training, whereas suboptimal training paradigms in fact reduce the transcriptional capacity of the cell by downregulating P-CREB. Future studies will determine whether this experience-dependent modulation of P-CREB and total CREB plays a role in boosting and blunting the effects of subsequent training.

https://doi.org/10.1038/s41467-024-53922-x

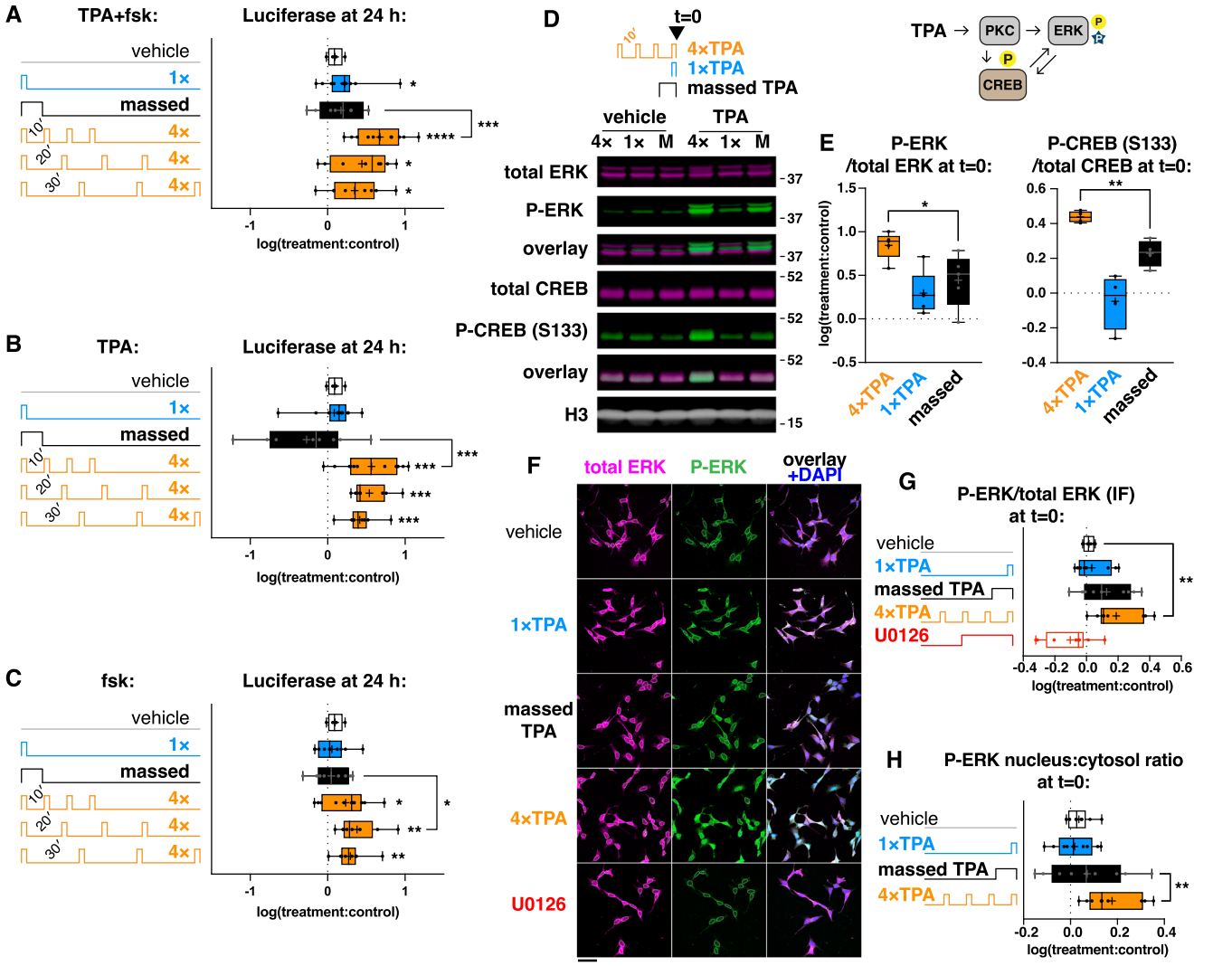

Fig. 3 | Massed-spaced effect in CRE-luc cells. A–C A combination of fsk and TPA (A), or either of the two agonists alone (B–C) were administered in various temporal patterns outlined on the left. Agonists were delivered either as a single pulse (1×3′), as a "massed" pulse (4 × 3′ without ITI), as four spaced pulses (4 × 3′, ITI = 10, 20, or 30 min). CRE-luc induction was measured 24 h from the onset of treatment. N represents independent experiments ($N = 4$ for Vehicle, $N = 11$ for 4×TPA+fsk (ITI 10 min), 4×fsk (ITI 10 min), 1×TPA+fsk and 1×fsk (including data from Fig. 2), $N = 12$ for 4×TPA (ITI 10 min) and 1×TPA, and $N = 8$ for the remaining data points). Asterisks by data bars indicate p values in two-tailed single-sample Student's t tests (Theoretical mean = 0; 1×TPA+fsk, $p = 0.0299$; 4×TPA+fsk (ITI 10 min), $p < 0.0001$; 4×TPA+fsk (ITI 20 min), $p = 0.0137$; 4×TPA+fsk (ITI 30 min), $p = 0.0244$; 4×TPA (ITI 10 min), $p = 0.0003$; 4×TPA (ITI 20 min), $p = 0.0004$; 4×TPA (ITI 30 min), $p = 0.0009$; 4×fsk (ITI 10 min), $p = 0.0199$; 4×fsk (ITI 20 min), $p = 0.0055$; 4×fsk (ITI 30 min), $p = 0.0048$). Asterisks between bars indicate p values in two-tailed paired Student's t tests (4×TPA+fsk (ITI 10 min) vs M TPA+fsk, $p = 0.0009$; 4×TPA (ITI 10 min) vs M TPA, $p = 0.0016$; 4×fsk (ITI 20 min) vs M fsk, $p = 0.0272$). See Fig. S2 for extended data. **D, E** Cells were lysed immediately following the 4×, 1× and massed TPA treatments and analyzed by Western blot. **D** Representative images showing levels of total and phospho-ERK and CREB at t = 0 following treatments shown above. Histone H3 was used as a loading control. Uncropped images are shown in Fig. S3. **E** Quantification of P-ERK/total ERK and P-CREB/total CREB ratios shown in (**D**). N represents independent experiments ($N = 5$ for P-ERK, $N = 4$ for P-CREB). Asterisks between bars indicate p values in two-tailed paired Student's t tests (P-ERK: 4×TPA vs M TPA, $p = 0.0438$; P-CREB: 4×TPA vs M TPA, $p = 0.0073$). **F** Representative immunofluorescent staining of total ERK (magenta) and P-ERK (green) in CRE-luc cells immediately after the same treatments as in (**D**). Same staining after treatment with U0126 for 30 min is shown in the bottom row. Nuclei are outlined based on DAPI signal included in the overlay in blue. Scale bar, 50 μm. **G** Quantification of ERK phosphorylation as shown in F, measured by immunofluorescence as a ratio of P-ERK to total ERK. $N = 9$ total biological replicates from 3 independent experiments. Asterisk indicates p value in a two-tailed paired Student's t test (Vehicle vs 4×TPA, $p = 0.08$). U0126 treatment represents the true baseline (see Fig. S5). **H** Quantification of nuclear-to-cytosolic ratio of P-ERK as shown in (**F**). Asterisk indicates p value in a two-tailed paired Student's t test (4×TPA vs M TPA, $p = 0.0055$). Summary p values: *$p < 0.05$; **$p < 0.01$; ***$p < 0.001$; ****$p < 0.0001$. Box-and-whisker plots show all values (points) with range (whiskers), interquartile range (box), median (center line) and mean ("+" sign within box). Source data are provided as a Source Data file.

Massed-spaced effect is blocked by ERK and CREB inhibition

To examine the role of ERK and CREB in mediating the massed-spaced effect, we employed U0126, the inhibitor of ERK phosphorylation, and 666-15, the inhibitor of CREB transcriptional activity[46,47]. Cells were preincubated with either inhibitor 10 min prior to the start of the training period. Drugs were maintained in the culture media throughout the training period and washed out either 1 h after the end of training (+1 h) or 24 h later upon sample collection (+24 h). Luciferase expression was measured at the 24 h time point by Western blot, together with total/phospho-ERK and CREB, with histone H3 used as loading control (Fig. 4A, S8–S15).

U0126 (10 μM) significantly reduced luciferase expression 24 h after 4×TPA treatment when the inhibitor was washed out 1 h after training (Fig. 4A). A 24 h hour treatment with U0126 actually elevated luciferase levels, but it also proportionately increased the expression baseline in cells treated with U0126 alone (Fig. S8), suggesting that

https://doi.org/10.1038/s41467-024-53922-x

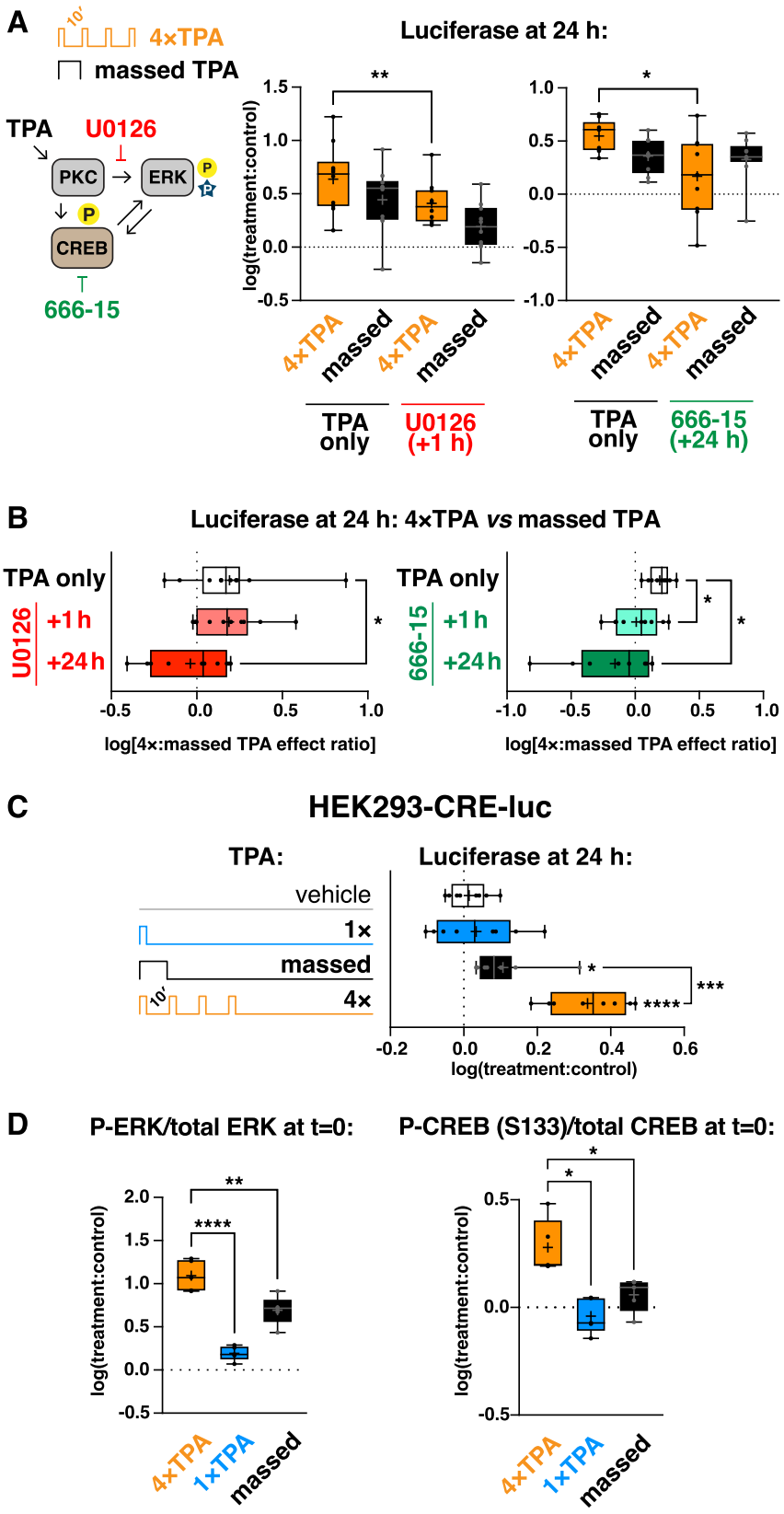

additional mechanisms may impact luciferase levels after such prolonged ERK inhibition—for example, the elevation could result from a reduction in proteasomal function, which would stabilize the PEST-tagged construct. Despite this confounding effect, we observed a progressive reduction in the ratio of luciferase induction by 4×TPA and massed protocols, suggesting that prolonged ERK activity helps support the massed-spaced effect. As expected, U0126 also strongly reduced ERK and CREB phosphorylation at 24 h (Fig. S9–10). U0126 did not affect total CREB levels at 24 h, although the elevation of total CREB in response to 4×TPA was still significant (Fig. S11).

666-15 (1 μM) also significantly reduced luciferase expression 24 h after 4×TPA treatment, both when the drug was washed out 1 h after

Fig. 4 | Mechanistic studies and generalization of the massed-spaced effect. **A** luc-CRE cells were treated with either 4× or massed TPA, and incubated in the presence of U0126 or 666-15 for 1 h or 24 h. Luciferase expression was measured 24 h after TPA treatment. *N* represents independent experiments (*N* = 10 for U0126; *N* = 9 for 666-15). Asterisks indicate *p* values in two-tailed paired Student's *t* tests (U0126: 4×TPA vs 4×TPA + U0126 1 h, $p = 0.0079$; 666-15: 4×TPA vs 4×TPA + 666-15 24 h, $p = 0.0166$). **B** Ratio of luciferase induction in (**A**), elicited by 4× or massed TPA treatments, with or without U0126 or 666-15. N represents independent experiments (*N* = 10 for U0126; *N* = 9 for 666–15). Asterisks between bars indicate p-values in a two-tailed paired Student's *t* test (U0126, left: TPA only vs U0126 24 h, $p = 0.029$) or Dunnett's post-hoc tests following repeated measures ANOVA (666-15, right: $F(1.489, 11.91) = 7.351$; $p = 0.0122$ for ANOVA; TPA only vs 666-15 1 h, $p = 0.0324$; TPA only vs 666-15 24 h, $p = 0.0242$ for Dunnett's tests). See Fig. S6–S10 for details and extended data. **C** HEK293 cells were stably transfected with the CRE-luc construct, and luciferase expression was measured 24 h after treatment with 1×, 4×, or massed TPA. Asterisks by data bars indicate *p* values in two-tailed single-sample Student's *t* tests (Theoretical mean = 0; M TPA, $p = 0.0136$; 4×TPA, $p < 0.0001$). Asterisks between bars indicate *p* value in a two-tailed paired Student's *t* test (4×TPA vs M TPA, $p = 0.0005$). *N* = 8 independent experiments. **D** HEK293 cells were lysed immediately after treatments as in (**C**) and analyzed by Western blot for P-ERK/total ERK and P-CREB/total CREB ratios. *N* = 5 independent experiments. Asterisks indicate *p* values in Dunnett's post hoc tests following repeated measures ANOVA (P-ERK: $F(1.795, 7.179) = 160.8$; $p < 0.0001$ for ANOVA; 4×TPA vs 1×TPA, $p < 0.0001$; 4×TPA vs M TPA, $p = 0.0039$ for Dunnett's tests. P-CREB: $F(1.943, 7.773) = 17.55$; $p = 0.0014$ for ANOVA; 4×TPA vs 1×TPA, $p = 0.0101$; 4×TPA vs M TPA, $p = 0.0229$ for Dunnett's tests). Summary *p* values: $^{*}p < 0.05$; $^{**}p < 0.01$; $^{***}p < 0.001$. Box-and-whisker plots show all values (points) with range (whiskers), interquartile range (box), median (center line) and mean ("+" sign within box). Source data are provided as a Source Data file.

training, and when maintained for 24 h (Fig. 4A, S12). Both treatments were sufficient to bring the ratio of luciferase induction by 4×TPA and massed protocols close to 1, completely blocking the spacing effect (Fig. 4B). Intriguingly, although 666-15 acts by preventing CREB binding to CBP[47], rather than CREB phosphorylation, we observed a significant decrease in the P-CREB(S133)/CREB ratio when cells were incubated with the inhibitor alone (Fig. S14), an effect apparently prevented by the TPA treatments. We also observed a significant reduction in total CREB levels in response to 666-15, when results from all conditions were averaged and compared to the average CREB levels in the absence of 666-15 (Fig. S15). This suggests that when CREB is prevented from binding to its targets, it is disproportionately dephosphorylated and possibly degraded, a dynamic that may provide one mechanism for cellular memory. Finally, a 24 h treatment with 666-15 caused a significant reduction in P-ERK levels after 4×TPA (Fig. S13), suggesting a positive feedback loop between sustained CREB-mediated transcription and ERK activity, which has indeed been reported[48]. To summarize, the sustained, interdependent activity of both ERK and CREB is required for the long-term induction of CRE-luc, and specifically by spaced training.

Massed-spaced effect is replicated in HEK293 cells

To verify that the effects described above were not due to neuron-like properties of neuroblastoma cells, we tested our findings in a different human cell line completely abstracted from the nervous system—HEK293 cells derived from embryonic kidney. We generated a stable monoclonal cell line based on HEK293, expressing the same CRE-luc construct used throughout this study. When subjected to TPA treatments (1×, 4×, and massed), these cells showed significantly stronger induction of luciferase at 24 h after the 4× spaced treatment compared to the other two paradigms (Fig. 4C). When HEK293 cells were treated in the same way and lysed immediately after treatment, the 4×TPA-treated cells also showed the expected disproportionate elevation in the P-ERK/total ERK and P-CREB/total CREB ratios compared to cells treated with massed TPA (Fig. 4D). Overall, HEK293 cells demonstrated a strong spacing effect, further generalizing our results.

Discussion

We have observed, in two separate non-neural CRE reporter cell lines, persistent (>24 h) transcriptional responses that discriminated between minute-scale time patterns of stimulation with activators of PKA and PKC. We showed that these responses depended on both the number of training pulses, and their precise temporal spacing, and that these factors determined not only the amplitude of the response but also the rate of its decay, demonstrating hallmark features of memory. These results show that behaviorally relevant features of cognition, such as the spacing effect and the forgetting curve, can be studied in dividing, non-neural cells. Our work therefore extends the concept of "cellular cognition" beyond neural systems, acknowledging that all cells must extract salient patterns from environmental signals and convert them into stable, longer-term responses[49].

Several cell signaling components have been previously implicated in such persistent, memory-like cellular responses and are likely to play a role in the effects observed here (Fig. S1). The activity of PKA can become persistent through the degradation of the enzyme's regulatory subunit[50]. PKC has multiple known mechanisms of persistence, including membrane insertion, proteolytic cleavage, and de novo synthesis of an atypical, constitutively active form of PKC termed PKM[51,52]. In the nervous system, these two kinases couple a large variety of neuromodulatory receptors (e.g. 5HT receptors, metabotropic glutamate receptors, muscarinic acetylcholine receptors, dopamine receptors, and β-adrenergic receptors) to the activation of ERK[43], whose persistence can be maintained through a number of mechanisms, including positive feedback at the cascade level, and a distributed mechanism of phosphorylation/dephosphorylation[20,21,24,53]. The transcriptional activity of CREB can also be persistently maintained. Known mechanisms include (i) a positive feedback loop involving the CREB-dependent production of a CREB-activating secreted messenger such as BDNF[48,54]; (ii) the degradation of transcriptional repressor ATF4/CREB2, known to depend on its phosphorylation of PKA[55]; and (iii) the stabilization of CREB output through CREB regulated transcription coactivator 1 (CRTC1), which can sustain CREB-dependent transcription independently of CREB phosphorylation[39,40]. All these mechanisms are likely to be highly integrated.

Our reporter system presents an opportunity to unravel the precise temporal relationships between the components of this complex, dynamic signaling network underlying learning and memory. An experimental throughput required to generate formal, mathematical models of cell signaling in memory formation is nearly impossible to attain using neural systems, including cultures of primary or iPSC-derived neurons. Our system, however, is infinitely scalable and could potentially be automated. This now enables us to pursue formalized molecular models of memory formation, with potential applications in cognitive enhancement and treatment of cognitive disabilities.

Our future research will focus on examining how global patterns of cell signaling, induced in response to training, predict specific memory outcomes. For example, in *Aplysia*, an unevenly spaced learning protocol designed to maximize interactions between PKA and ERK has been shown to enhance learning and even rescue learning deficits[56]. Similarly, insights gained using our reporter system could be applied to a wide range of real-life learning examples.

Methods

Reagents

Forskolin was from Amsbio. TPA was from CST. 666-15 was from Tocris Bioscience. Other reagents were from Sigma unless indicated otherwise.

Cell culture and treatments

Cell lines were acquired from ATCC (SH-SY5Y: CRL-2266; HEK-293: CRL-1573). Cells were maintained in standard growth media according to ATCC recommendations. For experiments, cells were seeded in 6-well plates at 0.3×10^6 cells per well. 24 h before treatment, media were changed to serum-free. Treatments were performed using gentle perfusion with a needleless syringe/vacuum manifold to minimize mechanical disruption and maintain stable temperature and pH. Drugs were dissolved in DMSO as 1000x stocks and diluted in serum-free media to a final DMSO concentration of 0.1% (referred to as "Vehicle" throughout), applied in precisely timed pulses, and washed out with vehicle-containing media.

Stable transfection

To generate the CRE-luc reporter cell lines, SH-SY5Y or HEK293 cells were transfected with pGL4.29[luc2P/CRE/Hygro] vector (Promega) using Lipofectamine 3000. Stable transfectants were selected using 200 μg/ml hygromycin. Monoclonal lines were isolated using the "scratch-and-sniff" method[57] and tested for luciferase induction in response to forskolin treatment.

Western blot

Cells were lysed in RIPA buffer with protease and phosphatase inhibitors (Roche). Western blotting was performed using standard protocols. Primary antibodies used: anti-P-ERK (CST #9101, polyclonal, 1:1000, lot 32), anti-ERK (CST #4696, L34F12, 1:1000, lot 33), anti-P-CREB (CST #9198, 87G3, 1:1000, lot 19), anti-CREB (CST #9104, 86B10, 1:1000, lot 8), anti-firefly luciferase (Invitrogen PA5-32209, polyclonal, 1:1000, lot ZF4348385), anti-β-actin (CST #3700, 8H10D10, 1:5000, lot 21), anti-H3 histone (CST #4499, D1H2, 1:10,000, lot 9). LiCor IRDye secondary antibodies were used at 1:10,000 dilution. LiCor ODM-0194 with LiCor Image Acquisition Software 1.1, was used for detection, and LiCor ImageStudioLite 5.0 software for densitometry analysis.

Luciferase assay

Luciferase activity was measured using the Luciferase Assay System (Promega) according to the manufacturer's instructions. Luminescence was measured using a Spectramax ID3 plate reader, and data collected using SoftMax Pro 7.1 software. Alternatively, luciferase levels were quantified by Western blot using an anti-luciferase antibody and normalized to β-actin or H3 histone as loading controls. Both methods were validated to produce highly correlated results (Fig. S16).

Immunofluorescence

Cells grown on laminin-coated coverslips were fixed with 4% formaldehyde, blocked, and incubated with primary antibodies (anti-P-ERK, CST #9101, 1:1000; anti-total ERK, CST #4696, 1:1000) overnight at 4 °C. Secondary antibodies (AlexaFluor 488 and 555, Thermo Fisher, 1:1000) were applied for 2 h at room temperature. Coverslips were mounted using ProLong Gold with DAPI (Thermo Fisher) and imaged using a Leica SP8 confocal system equipped with Leica Application Suite 3.5.5.19976 software. Images were analyzed using CellProfiler 4.2.5.

Statistics and reproducibility

All reported measurements were taken from distinct samples. Experiments were performed at least three times using a single replicate of each condition per experiment, except in calibration experiments reported in Fig. 2B–C (specific N numbers are provided for each data point). N numbers represent independent experiments, except in Fig. 3F–H, where $N = 9$ represents 3 biological replicates from 3 immunofluorescence experiments (treating these replicates equivalently to separate experiments did not result in a significant differences in variance compared to Western blot analysis (Fig. 3E) drawn only from independent experiments, as assessed using the Brown-Forsythe test). GraphPad Prism 10.3 was used for statistical analysis, with specific tests indicated in figure legends and Source Data. Data are presented as log of the ratio of the effect in the treated sample to that in untreated controls. Normal distribution was verified using the Kolmogorov-Smirnov test, and paired parametric statistics used throughout. No data were excluded from analysis. No statistical method was used to predetermine sample size. The experiments were not randomized, and investigators were not blinded to allocation during experiments due to the inherent constraints of the system (manual timing of pulses being the key independent variable, and all experimental samples in each experiment being derived from a single stock of cells). Investigators were blinded to conditions when analyzing Western blots and immunofluorescence images.

Reporting summary

Further information on research design is available in the Nature Portfolio Reporting Summary linked to this article.

Data availability

Source data are provided with this paper.

References

1. Cattaneo, V., San Martin, A., Lew, S. E., Gelb, B. D. & Pagani, M. R. Repeating or spacing learning sessions are strategies for memory improvement with shared molecular and neuronal components. *Neurobiol. Learn. Mem.* **172**, 107233 (2020).
2. Michael, D. et al. Repeated pulses of serotonin required for long-term facilitation activate mitogen-activated protein kinase in sensory neurons of Aplysia. *Proc. Natl Acad. Sci. USA* **95**, 1864–1869 (1998).
3. Carpenter, S. K., Cepeda, N. J., Rohrer, D., Kang, S. H. K. & Pashler, H. Using spacing to enhance diverse forms of learning: Review of recent research and implications for instruction. *Educ. Psychol. Rev.* **24**, 369–378 (2012).
4. Ojea Ramos, S., Andina, M., Romano, A. & Feld, M. Two spaced training trials induce associative ERK-dependent long term memory in Neohelice granulata. *Behavioural Brain Res.* **403**, 113132 (2021).
5. Wu, G. Y., Deisseroth, K. & Tsien, R. W. Spaced stimuli stabilize MAPK pathway activation and its effects on dendritic morphology. *Nat. Neurosci.* **4**, 151–158 (2001).
6. Ajay, S. M. & Bhalla, U. S. A role for ERKII in synaptic pattern selectivity on the time-scale of minutes. *Eur. J. Neurosci.* **20**, 2671–2680 (2004).
7. Anderson, M. J., Jablonski, S. A. & Klimas, D. B. Spaced initial stimulus familiarization enhances novelty preference in Long-Evans rats. *Behav. Process.* **78**, 481–486 (2008).
8. Menzel, R., Manz, G., Menzel, R. & Greggers, U. Massed and spaced learning in honeybees: The role of CS, US, the intertrial interval, and the test interval. *Learn Mem.* **8**, 198–208 (2001).
9. Mauelshagen, J., Sherff, C. M. & Carew, T. J. Differential induction of long-term synaptic facilitation by spaced and massed applications of serotonin at sensory neuron synapses of Aplysia californica. *Learn Mem.* **5**, 246–256 (1998).
10. Sisti, H. M., Glass, A. L. & Shors, T. J. Neurogenesis and the spacing effect: Learning over time enhances memory and the survival of new neurons. *Learn. Mem.* **14**, 368–375 (2007).
11. Ebbinghaus, H. *Memory: A contribution to experimental psychology*. (Dover, 1964).
12. Naqib, F., Sossin, W. S. & Farah, C. A. Molecular determinants of the spacing effect. *Neural Plast.* **2012**, 581291 (2012).

13. Pagani, M. R., Oishi, K., Gelb, B. D. & Zhong, Y. The phosphatase SHP2 regulates the spacing effect for long-term memory induction. *Cell* **139**, 186–198 (2009).
14. Philips, G. T., Tzvetkova, E. I. & Carew, T. J. Transient mitogen-activated protein kinase activation is confined to a narrow temporal window required for the induction of two-trial long-term memory in Aplysia. *J. Neurosci.* **27**, 13701–13705 (2007).
15. Philips, G. T., Ye, X., Kopec, A. M. & Carew, T. J. MAPK establishes a molecular context that defines effective training patterns for long-term memory formation. *J. Neurosci.* **33**, 7565–7573 (2013).
16. Kukushkin, N. V., Tabassum, T. & Carew, T. J. Precise timing of ERK phosphorylation/dephosphorylation determines the outcome of trial repetition during long-term memory formation. *Proc. Natl. Acad. Sci.* **119**, e2210478119 (2022).
17. Miranda, P., Mirisis, A. A., Kukushkin, N. V. & Carew, T. J. Pattern detection in the TGFβ cascade controls the induction of long-term synaptic plasticity. *Proc. Natl Acad. Sci.* **120**, e2300595120 (2023).
18. Kaang, B. K., Kandel, E. R. & Grant, S. G. Activation of cAMP-responsive genes by stimuli that produce long-term facilitation in Aplysia sensory neurons. *Neuron* **10**, 427–435 (1993).
19. Bhalla, U. S. & Iyengar, R. Emergent properties of networks of biological signaling pathways. *Science* **283**, 381–387 (1999).
20. Huang, C.-Y. & Ferrell, J. E. Ultrasensitivity in the mitogen-activated protein kinase cascade. *Proc. Natl. Acad. Sci.* **93**, 10078–10083 (1996).
21. Xiong, W. & Ferrell, J. E. A positive-feedback-based bistable 'memory module'that governs a cell fate decision. *Nature* **426**, 460–465 (2003).
22. Murphy, L. O., Smith, S., Chen, R.-H., Fingar, D. C. & Blenis, J. Molecular interpretation of ERK signal duration by immediate early gene products. *Nat. Cell Biol.* **4**, 556–564 (2002).
23. Smolen, P., Baxter, D. A. & Byrne, J. H. Bistable MAP kinase activity: A plausible mechanism contributing to maintenance of late long-term potentiation. *Am. J. Physiol.-Cell Physiol.* **294**, C503–C515 (2008).
24. Markevich, N. I., Hoek, J. B. & Kholodenko, B. N. Signaling switches and bistability arising from multisite phosphorylation in protein kinase cascades. *J. cell Biol.* **164**, 353–359 (2004).
25. Smolen, P., Zhang, Y. & Byrne, J. H. The right time to learn: Mechanisms and optimization of spaced learning. *Nat. Rev. Neurosci.* **17**, 77–88 (2016).
26. Farah, C. A., Weatherill, D., Dunn, T. W. & Sossin, W. S. PKC differentially translocates during spaced and massed training in Aplysia. *J. Neurosci.* **29**, 10281–10286 (2009).
27. Braha, O., Edmonds, B., Sacktor, T., Kandel, E. R. & Klein, M. The contributions of protein kinase A and protein kinase C to the actions of 5-HT on the L-type Ca2+ current of the sensory neurons in Aplysia. *J. Neurosci.* **13**, 1839 (1993).
28. Shuzo, S., Douglas, A. B. & John, H. B. Modulation of a cAMP/protein kinase A cascade by protein kinase C in sensory neurons of Aplysia. *J. Neurosci.* **17**, 7237 (1997).
29. Ghirardi, M. et al. Roles of PKA and PKC in facilitation of evoked and spontaneous transmitter release at depressed and non-depressed synapses in Aplysia sensory neurons. *Neuron* **9**, 479–489 (1992).
30. Braha, O. et al. Second messengers involved in the two processes of presynaptic facilitation that contribute to sensitization and dishabituation in Aplysia sensory neurons. *Proc. Natl Acad. Sci.* **87**, 2040–2044 (1990).
31. Yin, J. C. P. & Tully, T. CREB and the formation of long-term memory. *Curr. Opin. Neurobiol.* **6**, 264–268 (1996).
32. Suzuki, A. et al. Upregulation of CREB-mediated transcription enhances both short-and long-term memory. *J. Neurosci.* **31**, 8786–8802 (2011).
33. Silva, A. J., Kogan, J. H., Frankland, P. W. & Kida, S. CREB and memory. *Annu Rev. Neurosci.* **21**, 127–148 (1998).
34. Shaywitz, A. J. & Greenberg, M. E. CREB: A stimulus-induced transcription factor activated by a diverse array of extracellular signals. *Annu. Rev. Biochem.* **68**, 821–861 (1999).
35. Sun, W. et al. Spatial transcriptomics reveal neuron–astrocyte synergy in long-term memory. *Nature* **627**, 374–381 (2024).
36. Kukushkin, N. V. & Carew, T. J. Memory takes time. *Neuron* **95**, 259–279 (2017).
37. Wu, G. Y., Deisseroth, K. & Tsien, R. W. Activity-dependent CREB phosphorylation: Convergence of a fast, sensitive calmodulin kinase pathway and a slow, less sensitive mitogen-activated protein kinase pathway. *Proc. Natl. Acad. Sci. USA* **98**, 2808–2813 (2001).
38. García-Alai, M. M. et al. Molecular basis for phosphorylation-dependent, PEST-mediated protein turnover. *Structure* **14**, 309–319 (2006).
39. Conkright, M. D. et al. TORCs: Transducers of regulated CREB activity. *Mol. Cell* **12**, 413–423 (2003).
40. Uchida, S. et al. CRTC1 nuclear translocation following learning modulates memory strength via exchange of chromatin remodeling complexes on the Fgf1 gene. *Cell Rep.* **18**, 352–366 (2017).
41. Kolch, W., Calder, M. & Gilbert, D. When kinases meet mathematics: The systems biology of MAPK signalling. *FEBS Lett.* **579**, 1891–1895 (2005).
42. Pouyssegur, J. & Lenormand, P. Fidelity and spatio-temporal control in MAP kinase (ERKs) signalling. *Eur. J. Biochem.* **270**, 3291–3299 (2003).
43. Roberson, E. D. et al. The mitogen-activated protein kinase cascade couples PKA and PKC to cAMP response element binding protein phosphorylation in area CA1 of hippocampus. *J. Neurosci.* **19**, 4337–4348 (1999).
44. Hu, H.-J. & Gereau, R. W. IV ERK integrates PKA and PKC signaling in superficial dorsal horn neurons. II. Modulation of neuronal excitability. *J. Neurophysiol.* **90**, 1680–1688 (2003).
45. Harding, A., Tian, T., Westbury, E., Frische, E. & Hancock, J. F. Subcellular localization determines MAP kinase signal output. *Curr. Biol.* **15**, 869–873 (2005).
46. Xie, F. et al. Identification of a potent inhibitor of CREB-mediated gene transcription with efficacious in vivo anticancer activity. *J. Med. Chem.* **58**, 5075–5087 (2015).
47. Li, B. X. et al. Systemic inhibition of CREB is well-tolerated in vivo. *Sci. Rep.* **6**, 34513 (2016).
48. Obrietan, K., Gao, X.-B. & Van Den Pol, A. N. Excitatory actions of GABA increase BDNF expression via a MAPK-CREB–dependent mechanism—a positive feedback circuit in developing neurons. *J. Neurophysiol.* **88**, 1005–1015 (2002).
49. Kukushkin, N. V. Taking memory beyond the brain: Does tobacco dream of the mosaic virus? *Neurobiol. Learn Mem.* **153**, 111–116 (2018).
50. Lignitto, L. et al. Control of PKA stability and signalling by the RING ligase praja2. *Nat. cell Biol.* **13**, 412–422 (2011).
51. Sacktor, T. C. et al. Persistent activation of the zeta isoform of protein kinase C in the maintenance of long-term potentiation. *Proc. Natl Acad. Sci.* **90**, 8342–8346 (1993).
52. Klann, E., Chen, S.-J. & Sweatt, J. D. Mechanism of protein kinase C activation during the induction and maintenance of long-term potentiation probed using a selective peptide substrate. *Proc. Natl. Acad. Sci.* **90**, 8337–8341 (1993).
53. Ferrell, J. E. Jr. & Machleder, E. M. The biochemical basis of an all-or-none cell fate switch in Xenopus oocytes. *Science* **280**, 895–898 (1998).
54. Tao, X., Finkbeiner, S., Arnold, D. B., Shaywitz, A. J. & Greenberg, M. E. Ca2+ influx regulates BDNF transcription by a CREB family

transcription factor-dependent mechanism. *Neuron* **20**, 709–726 (1998).
55. Smith, S. G., Haynes, K. A. & Hegde, A. N. Degradation of transcriptional repressor ATF4 during long-term synaptic plasticity. *Int. J. Mol. Sci.* **21**, 8543 (2020).
56. Zhang, Y. et al. Computational design of enhanced learning protocols. *Nat. Neurosci.* **15**, 294–297 (2011).
57. Karin, N. J. Cloning of transfected cells without cloning rings. *Biotechniques* **27**, 681–682 (1999).

Acknowledgements

This work was supported by NIH grant no. 1R01MH120300-01A1 (T.J.C.). We would like to thank Anastasiya Susha for technical assistance. We would like to thank the lab of Dr. Stanislav Shvartsman (Princeton University) for helpful discussions of the earlier version of this manuscript.

Author contributions

N.V.K. conceived the project and designed all experiments. N.V.K., R.E.C. and T.T. performed the experiments and analyzed data. N.V.K., R.E.C., T.T. and T.J.C. interpreted the data. N.V.K. wrote the manuscript. T.J.C. edited the manuscript.

Competing interests

The authors declare no competing interests.

Additional information

Supplementary information The online version contains supplementary material available at https://doi.org/10.1038/s41467-024-53922-x.

Correspondence and requests for materials should be addressed to N. V. Kukushkin or T. J. Carew.

Peer review information *Nature Communications* thanks the anonymous reviewers for their contribution to the peer review of this work. A peer review file is available.